

Supplementary Figures and Tables

Figure S1. Analysis of expression profile of the miR-959-964 cluster in small RNA libraries from different tissues. Heatmap represents Z-normalized frequencies of miRNAs abundance in total population of miRNAs whithin each tissue.

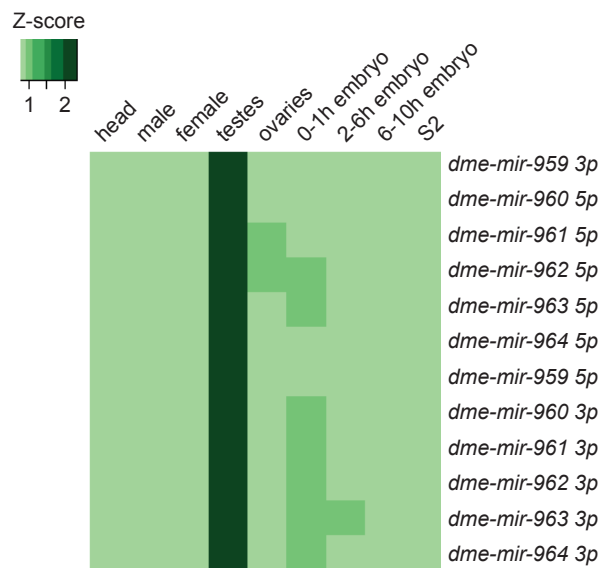


Figure S2. Deletion of the miR-959-964 results in male sterility.

(A) The scheme of the miR-959-964 deletion. (B) Fertility test of wild type and $\Delta miR-959-964$ males. (C) Fertility test of males with knockdown of CG31646 or CG18266 and carrying the mutation of CG31646. Control males of hp(CG31646) and hp(CG18266) strains carries transgenes with shRNA against genes while males of UAS/Dcr2+nos-GAL4 strain carries driver and helper Dcr2 transgenes; UAS/Dcr2+nos-Gal4+hp() carries both shRNA and driver. CG31646[MB09592] is males of 27790 strain from Bloomington Stock Center, carrying insertion of transgene in CG31646. (D) The effect of *MI03191* insertion within *miR-959-964* cluster on male fertility is dependent of the old age of males. Male fertility at (B), (C) and (D) refers to the average number of hatched progeny obtained from crossing of males of tested genotype with *Df(1)^{yw67c23(2)}* females.

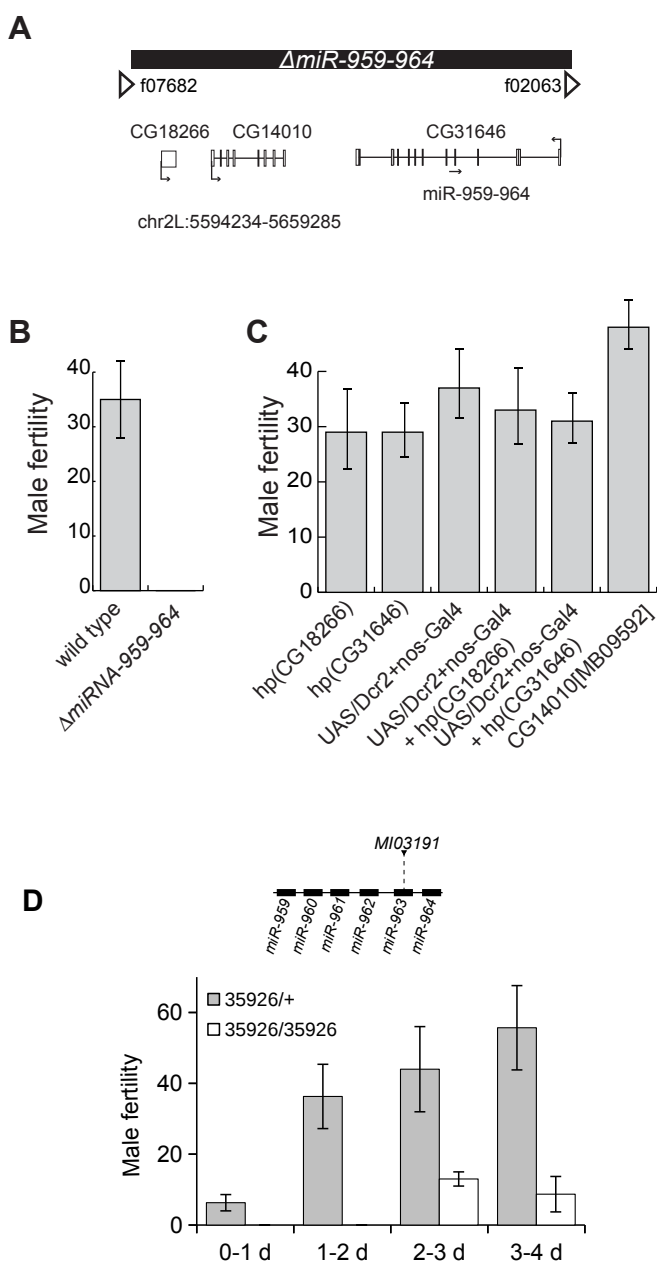


Figure S3. Phase-contrast images of wild-type and $\Delta miR-959-964$ testes.

(A) Post-mitotic mature primary spermatocytes with nuclei (arrow) and nucleoli (arrowhead).

(B) Post-meiotic round spermatids at the onion stage with nuclei (arrow) and Nebenkerns (arrowhead).

Scale bar, 10 μ m.

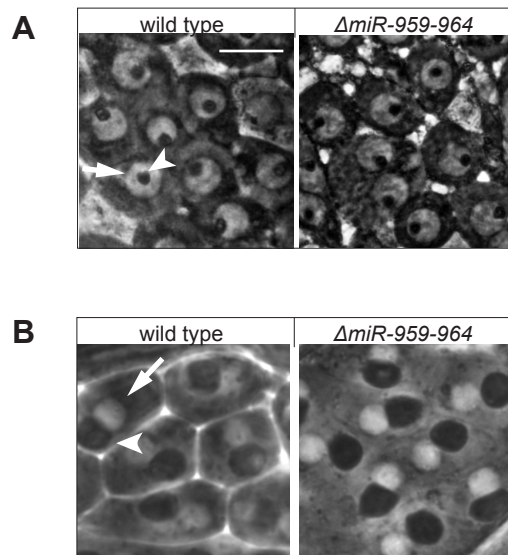


Figure S4. Testes of wild-type and *ΔmiR-959-964* males.

(A,B) The typical testis of a 3-day old wild type male. (C,D,E) The typical testis of a 3-day old *ΔmiR-959-964* male. (B,D and E) represent the magnification of the selected regions of testis as indicated at (A) and (C). Scale bar, 100 μ m (A,B) and 25 μ m (C,D,E). The spermatid nuclei are grouped in bundles in wild type testis while the spermatid nuclei of mutant testis demonstrate ‘scattered’ phenotype. Nuclei are stained by DAPI.

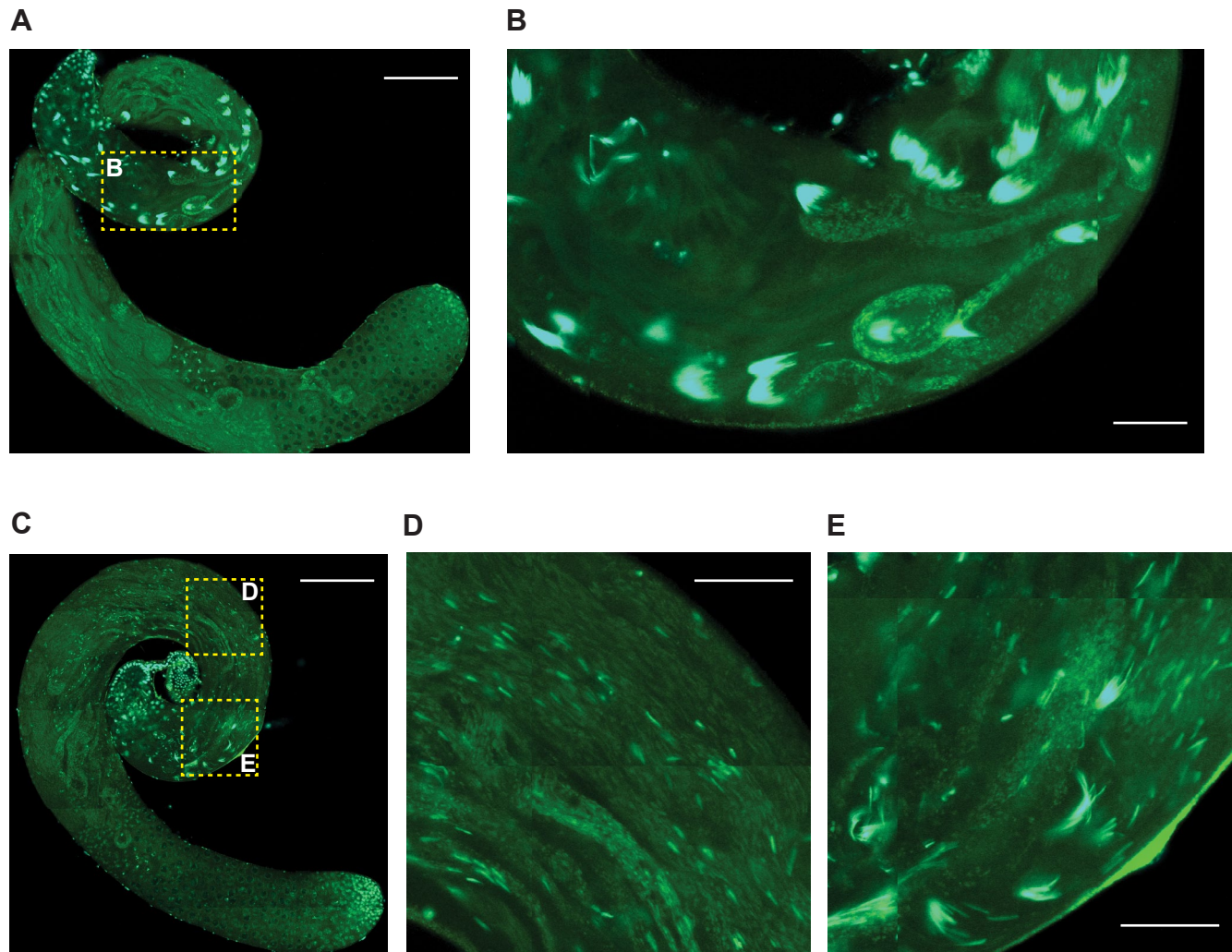


Figure S5. The novel putative miRNA in the miR-959-964 cluster.

(A) The location of novel putative pre-miRNA in miR-959-964. (B) The structure annotated alignment of novel pre-miRNA in different species evaluated by RNAalifold. The consensus secondary structure is present in dot-bracket notation. The minimum free energies (kcal/mol) and randfold *P*-values of pre-miRNAs are represented in the right panel. The significant *P*-values indicated the stable secondary structures are highlighted by gray color. (C) The MFE structure of novel putative pre-miRNA in *D. melanogaster* with unstable hairpin and *D. pseudoobscura* with stable hairpin drawing encode base-pair probabilities and evaluated by RNAfold.

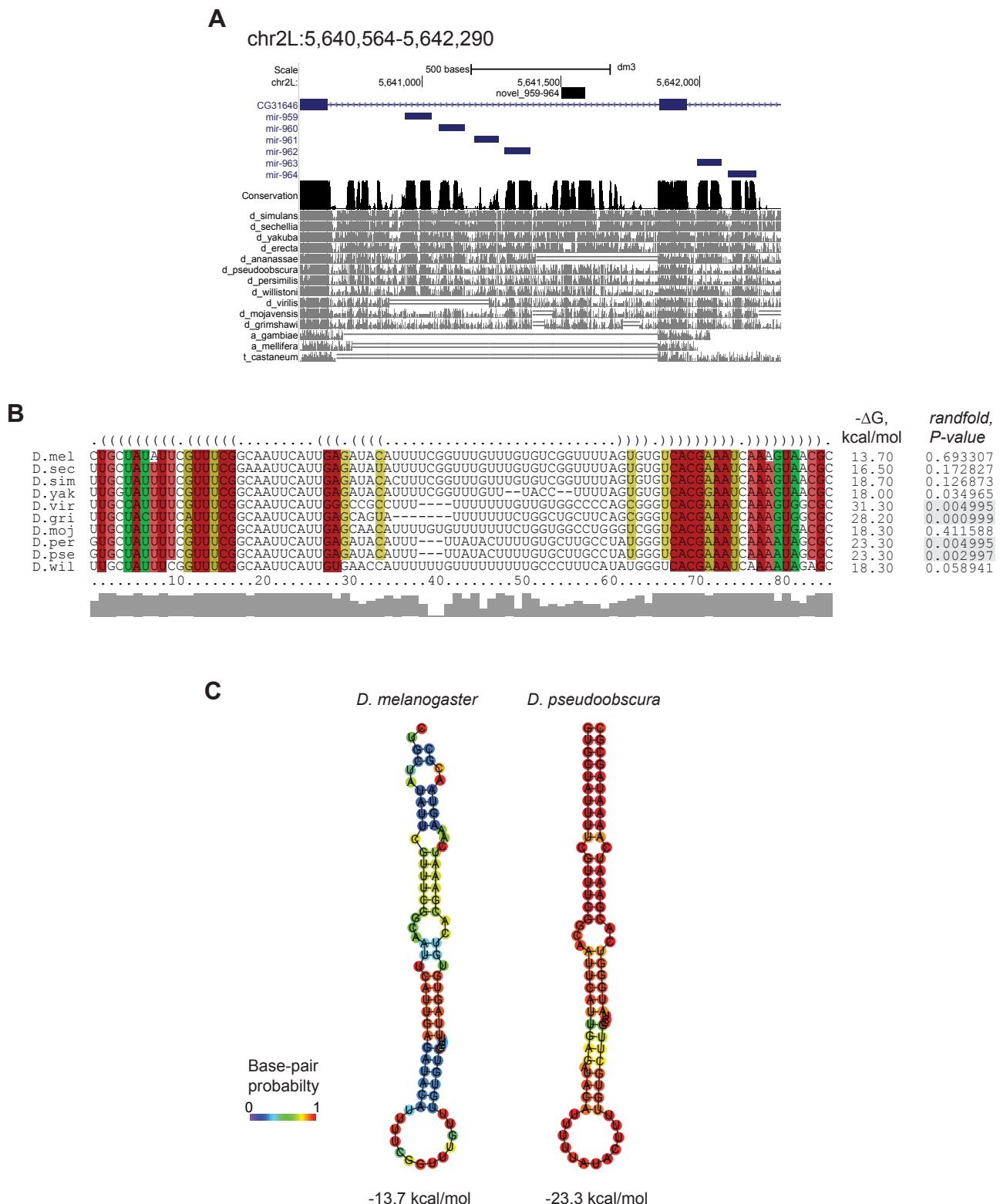


Table S1. Primers and probes used in this studies.

Primers for amplification of <i>miRNA-959~964</i> cluster		
clu_d	5'-ATGTATGCTAGCAGCCACGCAATCTAGGAGAAC	
clu_r	5'-TGGATTCTAGAGACCGATGCTCGATTTGTT	
Primers for amplification of 3'UTR fragments of genes		
didum-s	5'-TGGATTGGATCCACCGTCGCATCTTAATCTGG	
didum-as	5'-TGGATTGGATCCGTGGCTACCGGTATGGTGAC	
CG10033-s	5'-TGGATTCTAGAAGCAATGCCAGCAGTATCT	
CG10033-as	5'-TGGATTCTAGAATGTGCAACGCAATGAATT	
CG10512-s	5'-TGGATTCTAGAGCATTTGATGGACCAAAGC	
CG10512-as	5'-TGGATTCTAGAGTTGCAATCGCAAGAAAAAA	
CG1597-s	5'-TGGATTGGATCCATGCCACTTGACCACCTTCC	
CG1597-as	5'-TGGATTGGATCCGGAGCAGTACGATGACACCA	
CG33134-s	5'-TGGATTGGATCCCTAGATTGCTTGGGATCG	
CG33134-as	5'-TGGATTGGATCCTGCATAAACACCCAGACTTCG	
CG8824-s	5'-TGGATTCTAGAACATCGTGCACAAATGTCT	
CG8824-as	5'-TGGATTCTAGATGCAGGTGACGTTGAACACT	
CG8924-s	5'-TGGATTGGATCCCTAACGATCAGAAGCTGCAC	
CG8924-as	5'-TGGATTGGATCCAGTACTGGGGCGACAAGAAA	
Color legend:		
[ATGC]* - sequence added for improving the effectiveness of digestion		
[ATGC]* - restriction site of Nhe1		
[ATGC]* - restriction site of XbaI		
[ATGC]* - restriction site of BamH1		
After amplification, PCR-products were purified, digested by the corresponding restriction endonucleases and cloned in the vector as described in the Material and Methods section.		
Probes for Northern-blot		
anti-bantam	5'-ATCAGCTTCAAAATGATCTCA	
anti-miR-960*	5'-CtATgCAaTCTGGaATaCTCA	
*lowcase letters indicate LNA nucleotides		
Primers for screening of deletion (see also Parks et al, 2009)		
FDD_l-f	5'-CCCACAAACAAACCTCCAGAAC	Left genome-transgene junction
WH3' pl-ri-f	5'-CCTCGATATACAGACCGATAAAAC	Right genome-transgene junction
WH5' min r_f	5'-TCCAAGCGGCGACTGAGATG	
FDD_r_r	5'-AGCATAACCGGTCTTGATG	
Primers for RT-qPCR		
didum-s	5'-TTTCGTGCGTGGTGCTTG	
didum-as	5'-GATTCGCTGGTCTTGTGC	
CG10512-s	5'-CTCAGGATCCCAGTGGTGAA	
CG10512-as	5'-GAGTAGTTGGCTCCGGACAT	
fdl-s	5'-TCCCCAATCCCAGCCATTG	
fdl-as	5'-TCGCGCTACTATCCAGAGTT	
for-s	5'-GTTGCGACATGGTTGGGAG	
for-as	5'-ATGCATAACGTTGGGTGGC	

Table S1. Protein-coding genes with decreased level of expression in testis of $\Delta miRNA\text{-}959\text{-}964$. The adjusting of *P-value* for multiple hypothesis testing was performed wth Benjamin-Hochberg algoritm.

Name	logFC	P-value	P _{adj} -value
CG31601	-2.66	3.93E-06	2.45E-03
<i>Der-1</i>	-2.58	5.70E-06	2.68E-03
CG12376	-2.33	1.86E-05	4.85E-03
CG11455	-2.19	3.64E-05	7.77E-03
CG4631	-2.11	3.70E-06	2.45E-03
CG1380	-1.99	1.02E-04	1.19E-02
CG18808	-1.91	1.48E-04	1.66E-02
<i>Mst77F</i>	-1.88	2.13E-06	2.45E-03
<i>Peb</i>	-1.86	4.18E-06	2.45E-03
CG15109	-1.82	1.64E-05	4.85E-03
CG31788	-1.75	3.45E-04	2.47E-03
<i>Kap-alpha1</i>	-1.75	3.54E-04	2.47E-03
CG4714	-1.73	3.85E-04	2.51E-03
CG31286	-1.69	4.79E-04	2.88E-03
<i>PebII</i>	-1.64	6.63E-05	1.03E-02
CG11023	-1.63	6.55E-04	3.21E-02
CG8565	-1.63	1.82E-05	4.85E-03
CG8565	-1.58	8.57E-04	3.69E-02
CR33318	-1.57	7.04E-05	1.03E-02
CG31210	-1.52	3.20E-05	7.51E-03
CG10919	-1.51	1.26E-03	4.90E-02
CG17005	-1.51	1.29E-03	4.90E-02
CG14183	-1.50	9.98E-05	1.19E-02
Cul-3	-1.49	4.94E-05	9.05E-03
CG32371	-1.46	9.16E-05	1.19E-02
CG4706	-1.45	5.01E-05	9.05E-03
CG32081	-1.40	1.81E-04	1.77E-02
<i>Ran</i>	-1.39	7.02E-05	1.03E-02
CG5045	-1.29	3.59E-04	2.47E-03
CG13243	-1.28	3.44E-04	2.47E-03
<i>Psa</i>	-1.27	2.08E-04	1.88E-02
CG9254	-1.27	1.75E-04	1.77E-02
<i>Pen</i>	-1.27	1.74E-04	1.77E-02
<i>Npl4</i>	-1.26	3.36E-04	2.47E-03
<i>f-cup</i>	-1.25	6.37E-04	3.21E-02
CG31948	-1.24	2.45E-04	2.06E-02
<i>skap</i>	-1.22	5.87E-04	3.19E-02
CG4983	-1.21	5.38E-04	3.01E-02
CR40459	-1.21	4.68E-04	2.88E-02
<i>ssp5</i>	-1.13	5.35E-04	3.01E-02
<i>endos</i>	-1.13	7.09E-04	3.40E-02
<i>Porin2</i>	-1.11	6.49E-04	3.21E-02
CG15523	-1.11	1.11E-03	4.44E-02
CG7742	-1.09	9.74E-04	4.08E-02
CG4021	-1.09	7.45E-04	3.43E-02
CG3927	-1.07	8.65E-04	3.69E-02
CG43342	-1.05	1.08E-03	4.43E-02
CG9389	-1.02	1.29E-03	4.90E-02

Table S3. Genes Ontology terms enrichment of down-regulated genes in testis of $\Delta miR\text{-}959\text{-}964$. Top ten enriched terms for each category are represented. *P-values* were evaluated by Fisher's exact test and adjusted for multiple hypothesis correction with Benjamin-Hochberg ($P_{adj}\text{-value} \leq 0.05$).

Biological processes:

GO Term	<i>P-value</i>	<i>P_{adj}-value</i>	Number of genes
microtubule-based process [GO:0007017]	6.97E-06	3.89E-02	9
microtubule-based movement [GO:0007018]	2.29E-04		4
spermatid development [GO:0007286]	3.01E-04		4
sperm individualization [GO:0007291]	3.19E-04		3
spermatid differentiation [GO:0048515]	3.42E-04		4
spindle organization [GO:0007051]	5.83E-04		5
microtubule cytoskeleton organization [GO:0000226]	7.97E-04		6
protein complex subunit organization [GO:0071822]	2.10E-03		6
post-mating behavior [GO:0045297]	3.39E-03		2
spermatogenesis [GO:0007283]	3.42E-03		4

Cellular components:

GO Term	<i>P-value</i>	<i>P_{adj}-value</i>	Number of genes
cytoplasmic dynein complex [GO:0005868]	2.57E-07	2.33E-04	4
axonemal dynein complex [GO:0005858]	1.29E-07	2.74E-03	3
dynein complex [GO:0030286]	1.51E-05	2.93E-03	4
axoneme part [GO:0044447]	1.61E-05	2.99E-03	3
microtubule cytoskeleton [GO:0015630]	1.62E-05	3.66E-03	9
axoneme [GO:0005930]	1.98E-05	4.55E-03	3
microtubule associated complex [GO:0005875]	2.11E-05	5.86E-03	8
cytoskeleton [GO:0005856]	9.28E-05	1.05E-02	9
cytoskeletal part [GO:0044430]	2.97E-04	2.99E-02	8
cytoplasmic part [GO:0044444]	2.51E-03		15